EXTRACTION OF 3D SPATIAL POLYGONS BASED ON THE OVERLAPPING CRITERION FOR ROOF EXTRACTION FROM AERIAL IMAGES

Yair Avrahami [a] *, Yuri Raizman [b], Yerach Doytsher [a]

Department of Transportation and Geo-Information Engineering, Faculty of Civil and Environmental Engineering, Technion – Israel Institute of Technology.
[a] Technion City, Haifa 32000, Israel. (yaira, doytsher)@tx.technion.ac.il
[b] Survey of Israel, 1 Lincoln St., Tel-Aviv, 65220 Israel. yurirg@mapi.gov.il

KEY WORDS: Building extraction, Roof extraction, City model, Digital photogrammetry, Semi-automation, Aerial images

ABSTRACT:

This study presents algorithms for semi-automatic 3D spatial polygon extraction from a pair of colored aerial images with a known external model solution. The algorithm consists of several consecutive stages: initial pointing by a human operator which defines the algorithm as semi-automatic, extraction of a bounding polygon in the left image space, calculation of the estimated height and transformation to the right image space, extraction of a bounding polygon in the right image space and an iterative process which matches both polygons and extracts the spatial polygon. This algorithm is based on a 2D approach to solving the 3D reality and can be employed in many feature extraction situations. In this study, the algorithm is used for the spatial extraction of roofs and is presented in a semi-automatic interactive non model-based approach. In the proposed method, the operator needs to point at every distinct planar part of the roof in the left image space (2D). For each pointing, a specific roof plane is automatically extracted. The intersection of these planes provides us with the detailed roof structure. To examine the algorithm efficiency, a semi-automatic system for roof extraction was developed. The results we obtained were satisfactory and it appears that the algorithm can be implemented on many types of roofs and under diverse photographic conditions. This article presents the algorithm, the experiments and the results.

1. INTRODUCTION

Generating 3D city models is a relevant and challenging task, both from a practical and a scientific point of view (Gruen and Wang, 1998). This type of data is extremely important in many areas such as municipal management, planning, communications, security and defence, tourism, etc. It requires combination of the CAD and GIS systems where the spatial data must be stored in such a way that it can be queried and presented. Currently, GIS supports queries of 2D layers, where height information serves as one of many layer attributes. Joining the two systems can bring about the storage of 3D layers and the formulation of more complex queries for spatial analysis. Most of the input data for these systems is entered manually ("point by point") on Digital Photogrammetric Workstations (DPW).

This study presents algorithms for semi-automatic 3D spatial polygon extraction from a pair of colored aerial images with a known external model solution. The algorithm consists of several consecutive stages: 1) manual pointing to the center of a well-defined area in the left image space by an operator. This stage defines the algorithm as semi-automatic and from here on the process is fully automatic. 2) Segmentation of the area and extraction of its bounding polygon in the left image space. 3) Calculation of the estimated height and transformation of the initial pointing to the right image space. 4) Segmentation of the area and extraction of its bounding polygon in the right image space. 5) An iterative process which matches both polygons followed by extraction of the spatial polygon.

This algorithm is based on a 2D approach to solving the 3D reality and can be employed in many feature extraction situations. In this study, the algorithm is used for the spatial extraction of roofs and is presented in a semi-automatic interactive non model-based approach. In the proposed method, the operator needs to point at every distinct planar part of the roof in the left image space (2D). For each pointing, a specific roof plane is automatically extracted. The intersection of these planes provides us with the detailed roof structure. The proposed algorithm is beneficial in extraction of roofs since it is not confined to a specific model and therefore many different types of roofs may be extracted.

It is well accepted that the geometric data of roofs which are extracted manually or automatically are stored in one of the following ways: polyhedral models, prismatic models, parameterized polyhedral models and CSG models (Tseng and Wang, 2003). The proposed algorithm focuses more on the extraction of spatial data than on the storage method and so it can be modified to any one of the above mentioned categories.

In the course of this study a semi-automatic system for roof extraction from an aerial image was developed in order to examine algorithm efficiency. The results we obtained were satisfactory and it appears that the algorithm can be implemented on many types of roofs and under diverse photographic conditions. This paper is arranged in the following manner: Section 2 provides an overview of related work; Section 3 expands the algorithms for semi-automatic extraction of a single 3D spatial polygon; the next section demonstrates use of this algorithm for roof extraction, while the subsequent sections discuss the experiments (Sect. 5), results (Sect. 6), ending with the summary and conclusions (Sect. 7).

2. RELATED WORKS

The large amount of manual work required to extract roofs from aerial images has brought about the development of methods for automation of this area.

The automation methods vary and differ in the automation level offered. Usually, automation level is determined by the point of origin. In the automatic methods the initial pointings or the rough locations of the buildings are automatically extracted.

Cues such as color and DSM data have proved to be particularly valuable (Sibiryakov, 1996). In detection methods that exploit DSM or DEM data (Weidner and Forstner, 1995; Cord and Declercq, 2001; Ruther et al., 2002) the initial pointings or the rough locations are 3-dimensional. In other methods, they are 2-dimensional when using classification or texture analysis (Kokubu at al., 2001), shadow analysis (Irvin and McKoewn, 1989) or finding local maximums in a cumulative matrix of possible pointers (Croitoru and Doytsher, 2003).

Semi-automatic methods use initial data provided by the operator, such as pointing to or rough location of the building, or more detailed information such as 3-D point clouds, 3-D spatial lines in the roof, etc. There is a wide variety of algorithms for automation of building extraction in different areas (Gruen, 1997): types of buildings, required detail level, number of images, type of images cues and image primitives used, as well as external and a priori information utilized, automation level and operator intervention. This study focuses on developing semi-automatic algorithms whose sole input is a pair of colored aerial images with a known solution. The reason for focusing on this input derives from the intellectual challenge in this research area and from a practical point of view. The current algorithms which rely on this input only can be divided into two types: those that extract a contour and height of the roof (2.5-D mapping) and those that extract the detailed roof.

Oriot and Michel (2004) present a semi automatic approach for flat roof mapping. They suggest that the initial pointing would be 2D (i.e., on the left image) and performed manually. The rough location would be spotted by using Region Growing operations on the intensity and disparity images. The exact location and the matching of the images would be carried out using Hough Transform or Snake, according to the shape and the operator's decision. Ruther et al. (2002) focus on flat roof mapping in informal settlement areas and suggest extracting the rough location from the DSM. The exact location is extracted from an orthophoto using the Snake method.

Since creation of city-model data involves detailed extraction of elaborate roofs, it further complicates the problem. In order to scale-down the complexity and enable rapid and precise extraction, several methods which receive additional operator input operator were developed:

Gulch et al. (1999) proposed a building extraction system which is model-based and its automated features support the operator in adapting parametric models to multiple overlapping images. The operator's task is to fit to the images in monoscopic viewing a wire-frame model of the selected type. The operator needs at least two images in order to adjust for the correct absolute height. If only one image is available, other external information is required. Several possibilities exist in their study: purely manual adaptation, guided adaptation and automated adaptation.

Gruen and Wang (2001) proposed a semi automatic topology generator for 3D objects named "CC-Modeler". In order to extract a building, a 3D point cloud for each building must be generated. The cloud is composed of boundary points (BP), arranged in a clockwise or counter-clockwise topological order, and interior points (IP). From this point, the process is fully automatic and the CC Modeler assigns appropriate surfaces to the point cloud and generates the building topology.

Rau and Chen (2003) proposed a method, which is called "SPLIT-MERGE-SHAPE", for constructing building models using 3D line segments which are measured manually. The method comprises five major stages: the creation of the Region of Interest (ROI) and pre-processing, splitting the model to construct a combination of roof primitives, merging connected roof primitives, shaping each building rooftop and quality assurance. The amount of measurements in this method is of the same magnitude as that in the CC Modeler method, but this method has an advantage in that it also deals with partial lines and there is no need to estimate hidden corners.

Due to the complexity of automatic reconstruction of 3D reality from aerial images (occlusions, image quality, etc.), each method attempts in its own way to minimize the dependency on radiometric parameters of the image. The algorithms proposed in this study are based primarily on the radiometric parameters of the image and therefore can serve as a different approach to roof extraction (detailed below), or as an additional tool in current methods.

3. METHODOLOGY- SINGLE SURFACE EXTRACTION

In order to extract the roof of a building, the roof planes composing it must be extracted first. The following sections describe algorithms for extracting a spatial polygon (not only on a planar surface) where the input is a, initial 2D seed point in a typical radiometric area in the left image space. The working environment must be prepared prior to the extraction process. The pre-processing includes: model solution and image processing methods in order to emphasize the objects to be mapped. Following this stage, the automatic process consists of extraction in the left image space, calculation of the estimated average height, transformation to the right image, extraction in the right image, an iterative matching process based on overlapping areas between the polygons, identification of "real" homologous points and spatial mapping of the surface.

3.1 Left image operations

The purpose of this stage is to extract the area which was pointed out by the operator (the seed point) in the left image space (segmentation). The algorithm utilized in this study is based on Region Growing methods combining morphological operators ("open" and "close"), a Flood Fill operator and operators which eliminate "weak" and maintain "strong" edges. The entire segmentation process was carried out in the HSV color space, which enables good separation between colors. Following this process, the raster feature is converted to vector data using simplification methods, line adjustment and intersection with the outcome being an extracted polygon.

3.2 Approximate average height

A procedure for finding the homologous point is performed on every point of the extracted left polygon. The search for every point is performed on a specific area limited by geometric conditions: the epipolar-line equation and the possible

maximum and minimum building height. All points on the polygon in the left image represent edge points and are subjectively defined as "interest points". It would therefore be effective to use ABM (Area Based Matching) method for finding their homologous points.
The approximate average height is calculated by using the MEDIAN of the heights which has the highest value in the criterion for determining the optimal match.

3.3 Right image operations

After calculating average polygon height, it is possible to transfer the first seed point to the homologous point in the right image in two steps: transferring to local coordinates and from these to the right image space. It is performed by using the co-linear equation. From here on, the segmentation process around this point can be applied in the same way as in the left image. At the end of this process we obtain two polygons – one in the left image and one in the right image.

3.4 Left and Right polygon matching

Now that we have two polygons, homologous points between the two polygons are required to calculate the 3D spatial polygon. On the face of it, this is a simple process: for each point in the left polygon we can find the corresponding homologous point in the right polygon by intersecting the epipolar line and the right polygon. However, since extraction of polygons is performed automatically, the process often fails, such as when the number of points in both polygons is not equal, when there is an occlusion in one of the images and the polygons do not represent homologous areas, when there are a number of intersections per point, when a polygon line is parallel to the epipolar line, etc. To overcome these difficulties, an iterative method for maximal matching between the two polygons was developed. The matching process between both polygons is based on the well-known optimization model called "adjustment by conditions" (Cooper, 1987). The unknowns in this model are the heights of each point in the left polygon. The conditional equation (Equation 1) demands that after the left polygon is "transferred" to the right polygon (using height) maximum overlap (minimum difference between the interior and exterior areas) is created between the polygons in the right image space. First, the points in the left polygon are assigned the estimated average height, which was calculated previously. With each iteration these heights of points in the left polygon are updated until the conditional equation is optimized. During the iterations the left polygon "slides" in the direction of the epipolar line in the right image space. The "slide" rate is not constant because it depends on the varying height of each point. The iteration ("sliding") process stops when the polygons achieve maximum overlap in the right image space.

$$F = S_{out} - S_{in} \rightarrow \min \tag{1}$$

3.4.1 Pseudo-code of the iterative matching process

Algorithm 1 presents the pseudo-code of the main iterative matching process between the polygons in the right image space. In line (a) the left polygon is transferred (by the co-linear equation) to the right image space using the average estimated height (which was calculated in sec. 3.2). In line (b) the area of the interior polygon (resulting from Boolean intersection) and the external polygon (resulting from Boolean union) is calculated. Line (c) calculates the conditional function which is supposed to be minimized. Line (d) describes the partial derivative matrix, which is calculated in numerical fashion. Each matrix cell is a partial derivative of the conditional function for each point. In line (e) the corrections for the values from the former iteration is calculated according to the "adjustment by conditions" method.

In Figure 1 we can see the result of the matching process. The upper images show the left and right polygons. The lower left image shows the polygons after a single iteration and the lower right image shows the results after several iterations. Only after the matching process is completed, can we use an automatic process to extract homologous points in both polygons and reject "faulty" points which are found in the polygons but do not belong to the final surface result.

Algorithm 1: The pseudo-code for the iterative matching process between the polygons in the right image space is as follows (using the variables defined below):

Given:

$\{x_0, y_0, f\}, \{X_L, Y_L, Z_L, \omega_L, \varphi_L, \kappa_L\}, \{X_R, Y_R, Z_R, \omega_R, \varphi_R, \kappa_R\}$

$\{P_l\}_{1..i}$; $\{P_r\}_{1..j}$; $\overline{Z_G}$

Begin: Do until $(F \neq Min)$

(a) $P_l = \begin{Bmatrix} x_l \\ y_l \end{Bmatrix}_{1..i} + \{Z_G\}_{1..i} \Rightarrow \begin{Bmatrix} X_G \\ Y_G \\ Z_G \end{Bmatrix}_{1..i} \Rightarrow P_{l-r} = \begin{Bmatrix} x_{l-r} \\ y_{l-r} \end{Bmatrix}_{1..i}$

(b) $P_{l-r} = \begin{Bmatrix} x_{l-r} \\ y_{l-r} \end{Bmatrix}_{1..i}$; $P_r = \begin{Bmatrix} x_r \\ y_r \end{Bmatrix}_{1..j} \Rightarrow P_{out} = \begin{Bmatrix} x_{out} \\ y_{out} \end{Bmatrix}; P_{in} = \begin{Bmatrix} x_{in} \\ y_{in} \end{Bmatrix} \Rightarrow S_{out}; S_{in}$

(c) $F_{(Z)} = S_{out} - S_{in} = [b]$

(d) $B = \left[\frac{\partial F}{\partial (dZ_1)} \; \frac{\partial F}{\partial (dZ_2)} \; \frac{\partial F}{\partial (dZ_i)} \right] \Leftarrow \frac{\partial F_{(Z)}}{\partial (dZ_t)} = \frac{\left(F_{(Z_i+\varepsilon)} - F_{(Z)}\right)}{\varepsilon}$

(e) $dZ_{1..i} = -B^T \cdot \left(B \cdot B^T\right)^{-1} \cdot b$

(f) Update$(Z_{1..i}) \rightarrow Z_{1..i} = Z_{1..i} + dZ_{1..i}$;

End

variable definition can be found as following:

$\{x_0, y_0, f\}$ – The calibration parameters

$\{X_L, Y_L, Z_L, \omega_L, \varphi_L, \kappa_L\}$ – The left image external parameters

$\{X_R, Y_R, Z_R, \omega_R, \varphi_R, \kappa_R\}$ – The right image external parameters

$\{P_l\}_{1..i}$ – The left polygon

$\{P_r\}_{1..j}$ – The right polygon

P_{l-r} – The left polygon in the right image space

P_{out}, P_{in} – The interior and external polygons

S_{out}, S_{in} – The interior and external areas

$\overline{Z_G}$ – The approximate average height

F – The conditional function

b – The conditional function residual

B – The partial derivative matrix

$dZ_{1..i}$ – The corrections vector

3.5 Reconstruction of the 3D spatial contour

When the iterative process is converged and the two extracted polygons overlap each other in an optimal manner, homologous points can be found using a compatibility scheme. The process requires building an adjacency matrix between all points in both images and systematically extract the two closest points. When a pair of points are found they are deleted from the matrix and the process is repeated until all pairs have been found. Thus, we have a list of pairs sorted by minimum distance and all points which have no matching partners are automatically eliminated. From this list we select only those pairs that meet a user-defined criterion and these final points represent the 3D spatial polygon.

In the example in Figure 1, the polygon extracted from the left image is composed of 6 points whereas the polygon extracted from the right image is composed of 10 points. After the iterative matching process based in the maximum overlap criterion (Sec. 3.4) is complete it becomes easy to extract the spatial polygon which consists of only 5 nodes.

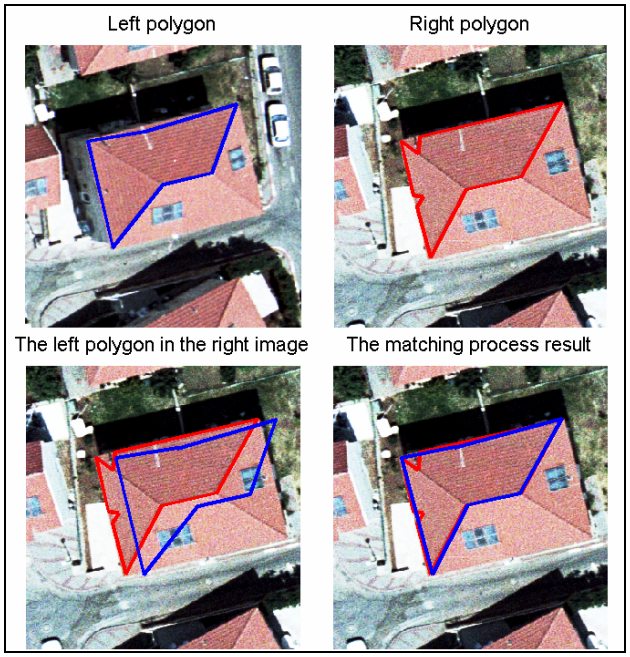

Figure 1. Result of the iterative matching process between the polygons in the right image space

4. ROOF EXTRACTION

In order to extract the roof of a building, the roof planes composing it must be extracted first. The proposed algorithm consists of three main stages: 1) Manual pointing - seed points (in 2D) to the centre area (in a typical radiometric point) of each roof plane in the left image space. 2) An automatic process for extraction of the roof planes for each seed point is performed. 3) Topology between the planes is built, the planes are intersected and the outcome is a 3D roof. Figure 2 illustrates a flowchart of the proposed algorithm.

Prior to the final stage we must ensure that each polygon in both images includes one seed point. If there are two or more pointers for a single polygon, then these pointers must be merged and consequently the areas which are represented by the pointers are also merged. Once the merging process occurs in one image, it must also be performed correspondingly in the other image. This case is very common and mainly caused by the different viewing angles of the aerial camera. The decision to merge and not split the polygons is derived from the fact that splitting requires information regarding the exact location of the split, whereas merging does not.

For example, in the lower-right roof in test area no. 2 (Figure 5) we can see that in the left image one polygon has been extracted for both the lower and right pointers of the roof. However, in the right image the same area has been extracted by two polygons – one for each pointer. And so, the 4 pointers in the lower right roof turn into 3 pointers and 3 polygons in both images. Another example can be found in the upper right roof which initially had 4 pointers that are converted into 2 pointers and 2 polygons only in both images.

Merging pointers and polygons in the image space results in creation of non-planar 3D polygons. Thus, each polygon must be checked for multiple sub-surfaces – whether the 3D spatial polygon is composed of more than one planar surface. If this is the case, the single 3D polygon is divided into several planar surfaces.

In the final stage, the topology between the roof planes is built up according to adjacent relationship between the lines composing the 3D planar polygons. Next, spatial intersection of adjacent planes is performed.

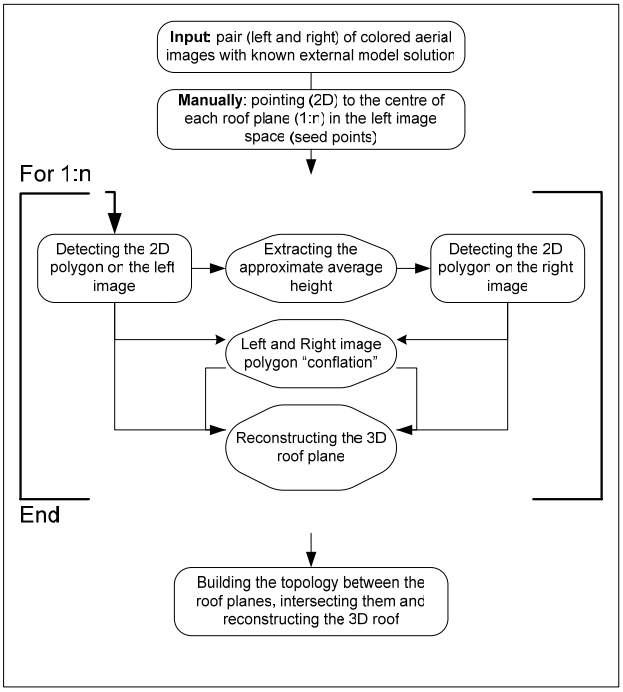

Figure 2. Flowchart of the roof extraction

5. IMPLEMENTATION AND EXPERIMENTS

In the course of research, a semi-automatic system for performing extraction from aerial images was developed using the MATLAB® environment, in order to examine the algorithm efficiency. The system enables performing manual pointing on the desired parts of the roof in the left image and automatic extraction of the 3D roof in a local coordinate system. The experiments were conducted on two test areas using aerial images scanned at a pixel size of 15μm. The first test area

(Figure 3) was medium scale 1:7500 and included eight roofs and the second (figure 5) was medium scale 1:5000 and included four roofs.

The aim of the tests was to examine the accuracy of the proposed semi-automatic extraction compared to the manual extraction and to assess the capabilities of the method with different types of roofs. Both areas contain 12 buildings with 3 roof types: front gabled (8 buildings in Test Area 1), which require 2 seed points – one for each aspect; pavilion-hipped (3 buildings in Test Area 2), which require 4 seed points; and a hybrid of the two types (the lower-left building in Test Area 2) which requires 3 seed points. The algorithm was tested twice (Test area 1 and Test Area 2) and the two parameters related to color disparity and spatial resolution were interchanged among the two tests. The first parameter is the region growing tolerance in each band of the HSV color space and the second is related to the simplification process. The parameters for every specific building in each area were not changed. Figures 3 and 5 show the extraction of polygons in the image space in test areas 1 and 2, accordingly. In addition, the initial manual (blue asterisk) is shown in the center of every polygon in the left image and the appropriate pointer in the right image, which was transferred automatically. Figures 4 and 6 present the extracted roofs in a local coordinate system in Test Areas 1 and 2, correspondingly. The presentation of walls and floors are for visualization purposes only. In order to generate walls and floors a point on the ground must be known or calculated form an appropriate DTM (not included in the input data).

The results of the extraction in Test Area 2 show how the algorithm overcomes problems such as a mismatch in the overlapping areas. In the left aspect in the upper-left building in Figure 5 we can see how the algorithm succeeded, despite the fact that in the right image the polygon included an additional "triangle", which does not belong to the desired 3D polygon. Since the left image did not contain the "triangle", the mutual polygon "conflation" scheme was able to dismiss this irrelevant part.

6. ANALYSIS OF THE RESULTS

In order to examine the accuracy of the results, the roofs were measured manually by an operator in the ERDAS IMAGINE 8.6® software. In the current research both mappings (manual and semi-automatic) were based on the same model solution with the same orientation errors and there is no need to take them into consideration.

The semi-automatic mapping accuracy was calculated based on the RMS [RMS=sqrt(sum(d*d)/n)] of the deviation vectors, between the two mappings, and on the evaluated accuracy of the manual mapping.

The deviation vector of each corner on the manual mapping and the closest corner on the semi-automatic mapping were measured. Altogether 48 deviation vectors belonging to 8 buildings in the first test area and 24 deviation vectors belonging to 4 buildings in the second test area were measured.

In Table 1, the RMS of the deviation vectors in the both test areas are presented. This RMS is a "compared" accuracy between the manual and the semi-automatic proposed mechanisms for mapping.

The accuracy of the manual mapping can be evaluated according to Kraus (1993) using Equations 2 and 3, where: m is the image scale, m_q is an estimation of the photogrammetric measurement's accuracy ($10\mu m$), Z is the flight height, and B is the base line. The semi-automatic mapping accuracy can be calculated according to the manual mapping accuracy and the "compared" accuracy by using Equation 4. The horizontal and vertical measurement accuracy in both test areas are presented in Table 1: the evaluated accuracy of the manual measurements (row 1); the RMS of the deviation vectors between the mappings (row 2); and the semi-automatic mapping accuracy (row 3).

$$M_{xy} = m \times m_q \tag{2}$$

$$M_z = m \times m_q \times \frac{Z}{B} \tag{3}$$

$$M^2_{semi-automatic} + M^2_{manual} = M^2_{compared} \tag{4}$$

Table 1. Horizontal and vertical measurement accuracy in both test areas (m).

	Accuracy (m)	Test area 1		Test area 2	
		H	V	H	V
1	Manual	0.08	0.13	0.05	0.09
2	Compared	0.17	0.39	0.11	0.22
3	Semi-automatic	0.16	0.37	0.10	0.20

Figure 3. Test Area 1 - Initial extraction in the left and right images

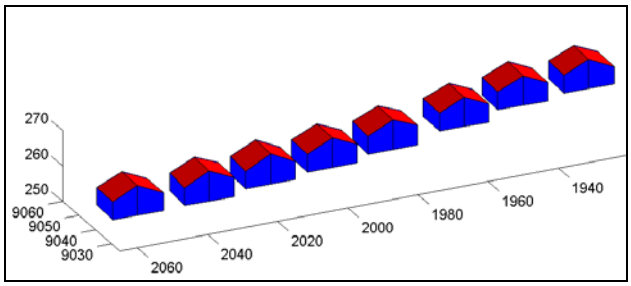

Figure 4. Test Area no. 1 - Roof extraction


Figure 5. Test Area 2 - Initial extraction in the images space

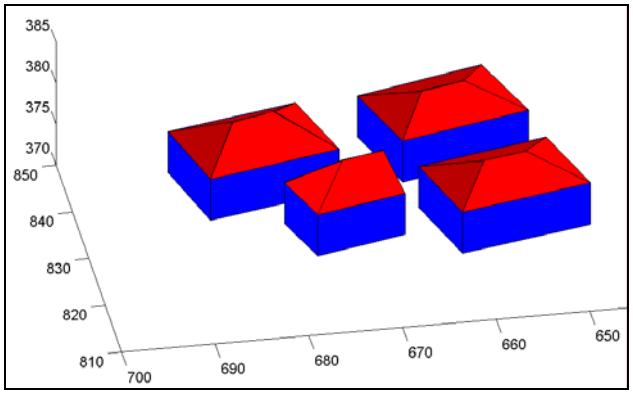

Figure 6. Test Area. 2 - Roof extraction

7. CONCLUSIONS

This study presents algorithms for semi-automatic extraction of 3D spatial polygons, based on an initial 2D manual pointing and their use for roof extraction. As can be seen, the accuracy of the semi-automatic extracted buildings was 16_{cm} in the horizontal direction for Test Area 1 and 10_{cm} in the horizontal direction for test area 2. The vertical accuracy was 37_{cm} in Test Area 1 and 20_{cm} in Test Area 2. The results show that using the developed semi-automatic method has achieved numerous advantages, namely: 1) rapid extraction of 3D building roofs from medium scale aerial images; 2) no restriction to specific roof types or models; 3) the mapping procedure is performed within a non-stereoscopic environment and without 3D spectacles; 4) this approach reduces the work required for roof extraction and thus is more economic; 5) the operator can identify at a glance which buildings can be mapped by this method so as to combine it with traditional manual extraction or the other semi-automatic method.

Additional research will focus on increasing accuracy of roof extraction and raising the success percentage by advances in fields such as developing an algorithm for management and combination of all information extracted from a single source - two aerial images. Greater automation of this algorithm may be achieved by finding automatic search methods for seed points to different parts of the roof. In this study we preferred to perform a semi-automatic algorithm in order to obtain higher accuracy and a higher success percentage.

8. REFERENCES

Cooper, M.A.R., 1987. *Control Surveys in Civil Engineering*, Collins, London, pp. 170-171.

Cord M. and Declercq D., 2001. Three Dimensional Building Detection and Modeling Using a Statistical Approach. *IEEE Transactions on Image Processing*, 10(5), pp: 715-723.

Croitoru A. and Doytsher Y., 2003. Monocular Right-Angle Building Hypothesis Generation in Regularized Urban Areas by Pose Clustering. *Photogrammetric Engineering & Remote Sensing*, 69(2), pp: 151–169.

Gruen A. and Wang X., 1998. CC-Modeler: A Topology Generator for 3-D City Models. *ISPRS Journal of Photogrammetry & Remote Sensing*, 53(5), pp: 286-295.

Gruen A. and Wang X., 2001. News from CyberCity Modeler.In: Automatic Extraction of Man-Made Objects from Aerial and Space Images (III), Balkema Publishers, Lisse, The Netherlands, pp: 93–101.

Gruen A., 1997. Automation in Building Reconstruction, In: Photogrammetrische Woche. Pages: 175-186. www.ifp.uni-stuttgart.de/publications/phowo97/gruen.pdf.

Gulch E., Muller H. and Labe T., 1999. Integration of Automatic Processes into Semi-Automatic Building Extraction. In: *International Archives of Photogrammetry and Remote Sensing*, Vol. (32) 3-2W5, pp: 177–186.

Irvin R.B. and McKeown D.M., 1989. Method for Exploiting the Relationship between Buildings and their Shadows in Aerial Imagery. *IEEE Transactions on Systems, Man, and Cybernetics*, 19(6), pp: 1564-1575.

Kokubu K., Kohiyama M., Umemura F. and Yamazaki F., 2001. Automatic Detection of Building Properties from Aerial Photographs Using Color and 3D Configuration. Presented at the 22nd Asian Conference on Remote Sensing, November 2001, Singapore.

Kraus, K., 1993. *Photogrammetry*, Vol.1, Duemmler, Bonn. pp. 231.

Oriot H., Michel A., 2004. Building Extraction from Stereoscopic Aerial Images. *Applied Optics*, 43(2), pp: 218-226.

Rau J.Y. and Chen L.C., 2003, Robust Reconstruction of Building Models from Three-Dimensional Line Segments. *Photogrammetric Engineering & Remote Sensing*, 69(2), pp: 181-188.

Ruther H., Martine H. and Mtalo E,G., 2002. Application of Snakes and Dynamic Programming Optimisation Technique in Modeling of Buildings in Informal Settlement Areas. *ISPRS* Journal of Photogrammetry & Remote Sensing, 56(4), pp: 269-282.

Sibiryakov A., 1996. House Detection from Aerial Color Images. *Internal Report, Institute of Geodesy and Photogrammetry*. Swiss Federal Institute of Technology, Zurich (ETH).

Tseng Y. and Wang S., 2003. Semiautomated Building Extraction Based on CSG Model. *Photogrammetric Engineering & Remote Sensing*, 69(2), pp: 171-180.

Weidner U. and Forstner W., 1995. Toward Automatic Building Reconstruction from High Resolution Digital Elevation Model. *ISPRS Journal of Photogrammetry & Remote Sensing*, 50(4), pp: 38-49.